Arch. Min. Sci. **70** (2025), 3, 505-523

Electronic version (in color) of this paper is available: http://mining.archives.pl

DOI: https://doi.org/10.24425/ams.2025.156296

W. DZIURZYŃSKI[1*], P. OSTROGÓRSKI[1], P. JAMRÓZ[1],
P. SKOTNICZNY[1], S. TRENCZEK[2]

MEASUREMENTS OF AIR-METHANE MIXTURE FLOW RATE IN MINE FAN DUCT: A COMPARATIVE STUDY

In this article, the results of a precise measurement of the volume flow rate of an air-methane mixture flowing out of a mine shaft are presented and compared with measurements at the air intakes to the shaft. Continuous measurement of the volume flux of the air-methane mixture in underground mine workings is a complex issue, and with the requirements for the determination of methane emissions by the mining company based on quantitative measurements of methane in the air discharged through the ventilation shaft, it is a topical and important issue for ecological and economic reasons. The development of measurement methods based on a purpose-built instrument was followed by the development of a system for the multipoint measurement of methane velocity and concentration, using SOM 2303-type methane anemometers. With the helpful cooperation of the mine, simultaneous measurements were taken in the collection duct of Shaft VI and at all four air intakes to the shaft. The results obtained were presented in the form of determined air and methane fluxes, followed by a comparison with the volume flux measurements taken in the workings of the inlet to Shaft VI.

Keywords: Underground mine; airflow and methane measurement; comparative study

1. Introduction

The introduction of the EU regulation (on the reduction of methane emissions in the energy sector and amending Regulation (EU) 2019/942 [25], in particular concerning the monitoring of methane emissions from coal mines, poses a challenge in terms of a precise method for monitoring the release of methane into the atmosphere from ventilation shafts of Polish mines [1,29,30].

[1] STRATA MECHANICS RESEARCH INSTITUTE OF THE POLISH ACADEMY OF SCIENCES, 27 W. REYMONTA STR., 30-059 KRAKOW, POLAND
[2] CENTRAL MINING INSTITUTE NATIONAL RESEARCH INSTITUTE, PL. GWARKÓW 1 40-166 KATOWICE, POLAND
* Corresponding author: dziurzyn@imgpan.pl

Monitoring air velocity is a crucial factor in assessing the safe ventilation of mine workings in accordance with mining regulations. Many researchers are interested in performing correct measurements of air flow velocity [3,4], and the presentation of measurement results in the form of a contour map of air flow velocity in the cross-sectional area provides useful information [8,31,33,34].

An increasing number of automatic measurement systems are being used in underground mines, especially air velocity [13,15,20] and methane concentration [17]. The modern capabilities of specialised measurement and recording equipment allow simultaneous measurements to be carried out by more than a dozen air flow velocity sensors in the cross-section of the mine working. Such measurements are intended to determine the volume flow of the air-methane mixture. Determining the volume flow of air and gases in mine workings, tunnels, and ducts is a complex measurement. The flow rate is calculated using the bulk velocity method, considering the boundary layer and the cross-sectional area of the mine working.

To determine the volumetric flow rate of air and methane, air velocity and methane concentration in the fan duct were measured. For many years, the authors of the present study have been researching the velocity of air flows in mine workings. Their goal has been to develop measuring devices and improve existing methods to enhance the accuracy of air flow and methane measurement. One of the measuring devices developed is the SOM2303, which in an assembly of around a dozen to 30 devices of this type, together with an instrument scaffold, forms the Multipoint Velocity Field Measurement System (SWPPP), enabling measurements to be taken and recorded at selected points in the working cross-section. It can be assumed that the use of the SWPPP system enables a reference measurement to be made and will provide a reference point for manual measurements made with an anemometer, e.g. using the traverse method in the cross-sectional area of the working.

In SWPPP, SOM2303-type methane anemometers are used, which have an integrated vane sensor with a methane sensor [18,19]. The SOM2303 instrument has EC type-ex certification: OBAC 14 ATEX 0266X. The lower measuring range of the speed sensor of 0.16 m/s is noteworthy. This is confirmed by a calibration certificate from an accredited calibration laboratory for ventilation measuring instruments, certificate no. AP-118.

The applied measurement of volume flow rate using the bulk velocity method is based on the integration of the velocity distribution in the cross-sectional area of the channel. For circular or rectangular cross-sections, the number and distribution of measurement points, as well as the method of calculating the flow rate, are defined by standards. The method of estimating the air velocity distribution using linear triangulation used in the measurements in question was published in the paper [13]. This method involves dividing the cross-sectional area into triangular or quadrangular areas such that the vertices of these shapes are the measuring points. In this way, it is possible to calculate the velocity distribution in the vicinity of the sidewall of the ventilation duct, which has been overlooked in methods to date. The use of multiple simultaneously measuring methane anemometers arranged on a specially designed truss at different points in the cross-sectional area of the working, combined with simultaneous recording of the measured values, makes it possible to accurately estimate the instantaneous distribution of air velocity in the cross-section and to calculate the value of the volume flow of air and methane instantaneously or over a set period of time.

In shaft VI in the mine, there is a three-ventilator station equipped with FAWENT fans. The main fan station consists of three WPG 240/1.4A centrifugal fans of the same performance built in parallel, with one fan as a reserve.

To determine the volumetric flow rate of air and methane, it was planned to carry out measurements of air velocity and methane concentration at the most convenient metrological location, i.e. in the 27-metre-long collecting duct of the three-ventilation main ventilation station, with the anticipated location of the measurement station being 8 meters from the end of the straight section of the duct. In the selected channel cross-section, 16 methane anemometers were placed in a special holder and attached to the truss, shown in (Photo 1).

For the study, the author's IZO-VM computer software was extended to include the ability to visualise the distributions of air velocity and concentration of methane flowing through the mine workings. The IZO-VM software makes it possible to calculate the working cross-section and the air and methane volume flux, including the boundary layer, by means of the velocity field method for selected measurement durations [13].

2. Results of volumetric airflow and methane measurements

After deploying 16 methane anemometers in the duct (Photo 1), they were switched on and started measuring flow velocity and methane concentration. The fan station operator then started the fan station for Shaft VI, with two fans operating in parallel. Measurements were taken continuously between 17:33 and 19:44. After the measurements, the values recorded were retrieved from the memory of the methane anemometers and saved as a datafile.

To observe and analyse the recording of air velocity and methane concentration for the measurement system using the IZO-VM software, [8], it is necessary to enter into the IZO-VM software the files saved at the measurement station (Photo 1), moreover, the dimensions of the working cross-section and the coordinates of the measurement points of the position of the

Photo 1. View of the measurement station in the collecting duct of shaft VI of the mine, enlarged view of SOM2303

methane anemometers were entered into the option “Working cross-section”. Geometric measurements were performed using a laser rangefinder, which results in a low level of uncertainty in the measurements.

As sensors can start recording measurements at different times, the IZO-VM software synchronises the recording time for all sensors at the observed site. Measurements were processed for the time interval during which all sensors were operating.

TABLE 1 shows the data entered for the dimensions of the working and the location of the measuring sensors; these are the coordinates of the measuring points recorded in the format „Sensor number x[i] y[i]“, where “i” is the sequence number of the sensor.

TABLE 1

Data on the dimensions of the working and the location of the measuring sensors

Mine gallery data

Mine: Szczyglowice | Test site no.: 1

Width of cross-section: 5.81

Height of cross-section: 4.96

Number of measurement points (sensors): 16 | Read

coordinates of measurement points

Point no.	Sensor ID	X [m]	Y [m]
1	18	3,65	4,36
2	19	3,65	3,13
3	20	0,65	3,18
4	21	2,15	4,39
5	22	2,14	1,83
6	24	2,15	3,15
7	25	5,15	4,33
8	26	0,65	4,38
9	27	5,19	1,84
10	29	5,15	3,16
11	30	3,65	0,68
12	31	2,15	0,59
13	32	0,65	0,55
14	33	5,15	0,64
15	35	0,63	1,85
16	37	3,68	1,81

After reading the measurement data, the top bar (Fig. 1) of the IZO-VM software lists the number of measurements read, as well as the date and initial recording time (from 17:33 to 19:44) of the measurement data for the site. Sixteen sensors were deployed in the cross-section of the working area, and measurements were taken over 132 minutes, with a total of 7,919 measurements.

Fig. 1. Top bar of the IZO-VM software

Using the IZO-VM program, the cross-sectional area of the measurement site was determined to be 28.82 m^2, and the thickness of the boundary layer of the flowing air, determined for the measurement conditions in the duct, was entered into the volume flow calculations [9,13,27]. In the developed application (IZO-VM), the TeeChart component integrated within the Delphi development environment is utilised to generate a velocity contour plot based on data acquired from each metanoanemometer of the SWPPP system. After importing the velocity data, the application processes the spatial distribution of air velocity across the measurement grid. The processed data is then interpolated onto a regular mesh. A key boundary condition was imposed: the air velocity is assumed to be zero along the perimeter of the measurement area. During the generation of the methane concentration contour plot, it was presumed that the concentration along the boundary is equal to that measured by the nearest methane sensor. As a result, the contour lines are perpendicular to the boundary. These assumptions were adopted during the contour plot generation process to ensure that the interpolation near the boundaries reflects realistic flow behaviour and adheres to physical constraints. The TeeChart component then visualises the results using a contour chart. This chart presents velocity magnitudes as continuous, colour polygonal chains, and methane concentrations as contour lines that either intersect the boundary or form closed polygonal shapes, depending on the spatial distribution of points with equal concentration. This approach facilitates a clear and intuitive interpretation of spatial variations in both airflow and gas concentration. Based on the recordings carried out with the IZO-VM software, isotachs of air flow velocity (Fig. 2) and isolines of methane concentration in the cross-sectional area of the collecting duct of the fan station (Fig. 3) were determined for the selected time instant of 17:50.

The following figures show graphs of the change in velocity and methane concentration over time, for an example of three sensors of the measurement system.

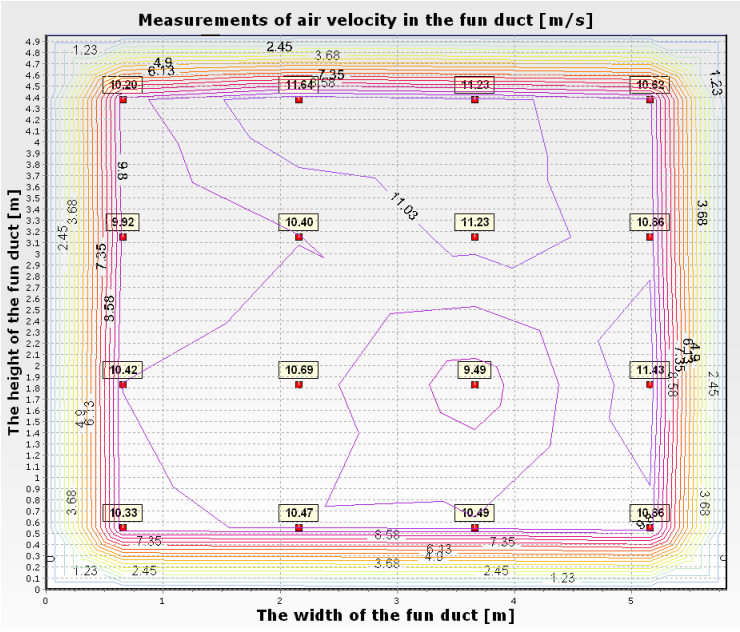

Fig. 2. Air velocity isotachs, time 17:50

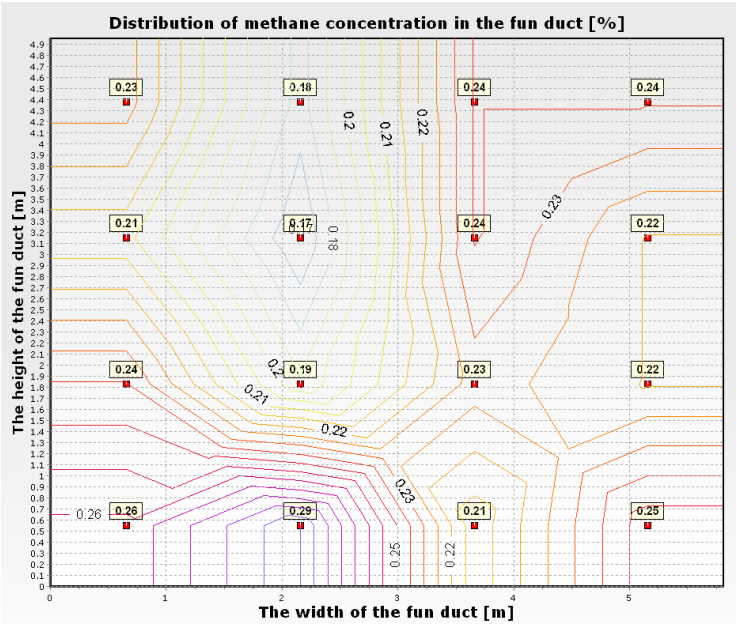

Fig. 3. Isolines of methane concentration in the flowing mixture, time 17:50

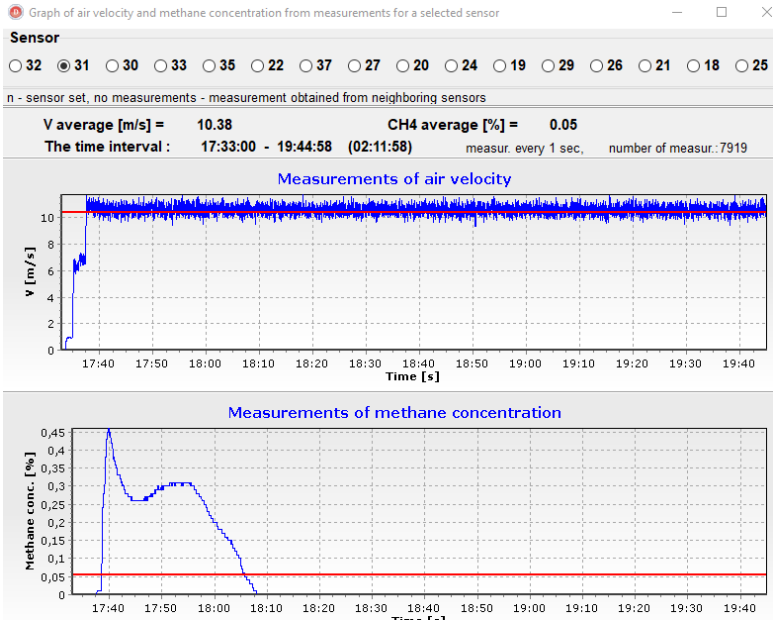

Fig. 4. Time diagrams for sensor no. 31, position x = 2.15; y = 0.59
top diagram – air flow velocities in the duct section, bottom graph – changes in methane concentration in the channel section

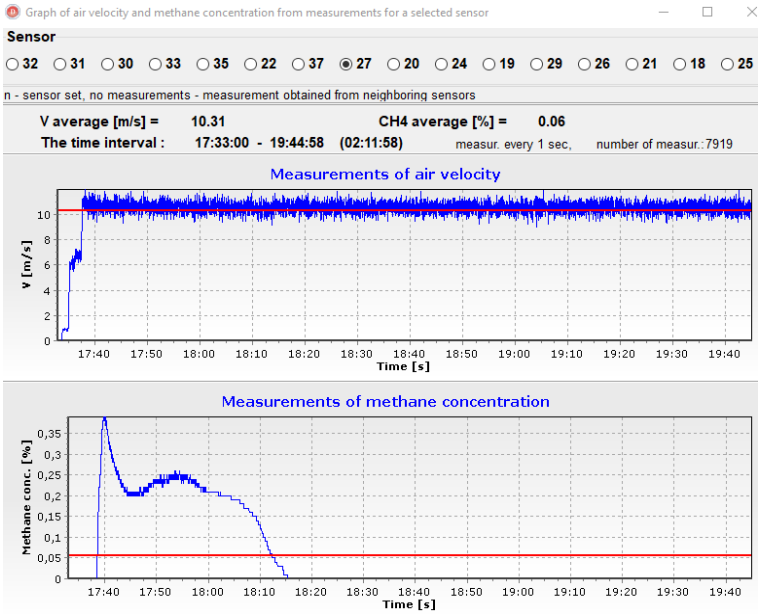

Fig. 5. Time diagrams for sensor no. 27, position x = 5.19; y = 1.84
top diagram – air flow velocities in the duct section, bottom graph – changes in methane concentration in the channel section

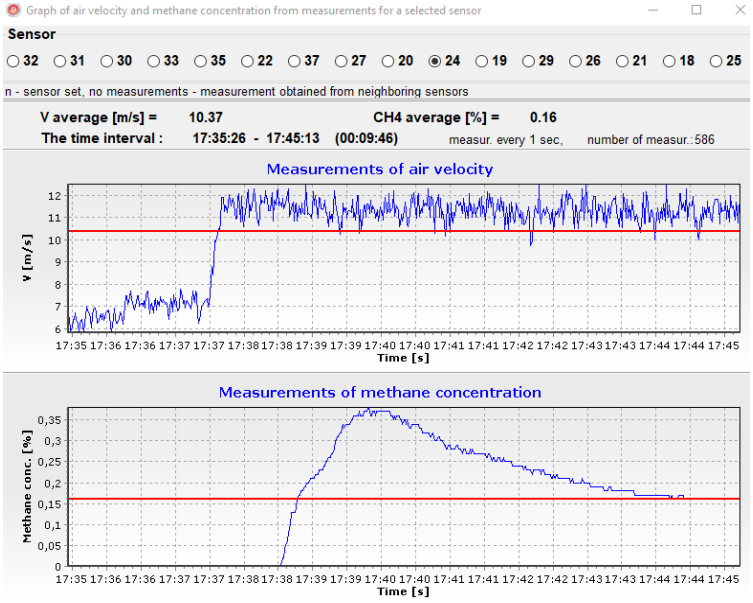

Fig. 6. Time diagrams for sensor no. 24, position x = 2.15; y = 3.15
top diagram – air flow velocities in the duct section, bottom graph – changes in methane concentration in the channel section

Analysing the obtained measurement results shown in Figs. 4, 5 and 6, we note that the methane concentration, after a momentary increase in concentration to a value of 0.4 to 0.45% CH_4, decreases and stabilises at a level of 0.25 to 0.35% CH_4 and, after several minutes, decreases to a value of 0.05% CH_4. The reason for this is the water vapour content of the air, the consequence of which is the phenomenon of water vapour condensing from the flowing air on the surface of the methane sensor. The sensors used in the SOM 2303 cannot operate in condensation conditions, as this is outside the humidity range of the methane sensor specified by the sensor manufacturer. In view of the above, the results of two air samples taken from the diffuser of shaft VI into Tedlar bags, whose gas concentration values were measured at the Gas Analysis Laboratory of the Department of Mining Aerology of the Central Mining Institute using a gas chromatograph, are used to determine the methane volume flux; TABLE 5 shows the results of the analyses performed.

Fig. 7 shows the average air flow rate in the duct cross-section, calculated from measurements, from 18:40:02 to 19:20:12. The calculated mean value of the flow was $Q_v = 296.77$ m^3/s (17806 m^3/min).

Commenting on the result obtained, it should be noted that the measurement method using the SWPPP system considers a correction for the determined value of the boundary layer, which is not included in the method using the anemometer traverse [23].

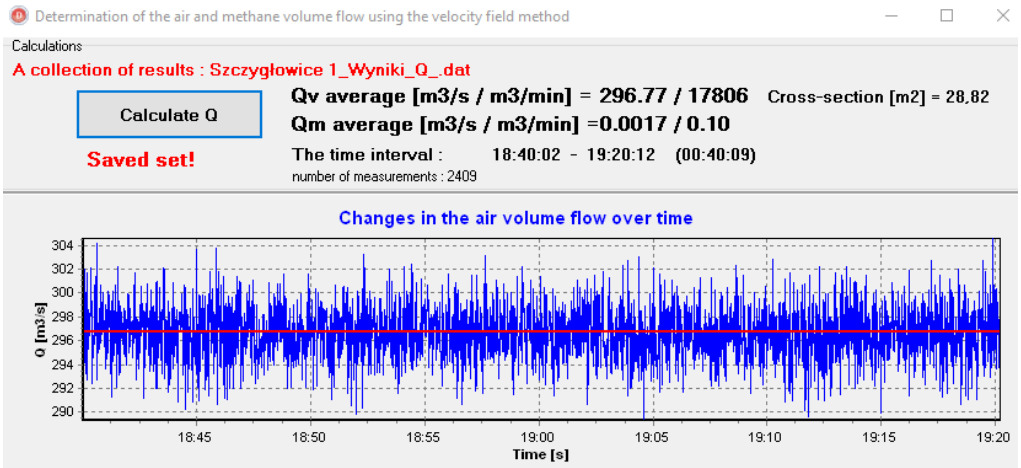

Fig. 7. Volume flow $Q_v = 296.77$ m^3/s; 17806 m^3/min, average value for the period 18:40:02 to 19:20:12

Based on the determined volume flow rate of the flowing air Q_v (Fig. 7) and from the data shown in TABLE 5, the volume flow rate of the $\dot{V}_i\,CH_4$ out through shaft VI was calculated according to the formula:

$$\dot{V}_i\,CH_4 = 0.01 \cdot Q_v \cdot q_i\,CH_4,\ [\text{m}^3/\text{min}] \tag{1}$$

where:

Q_v – air flow rate at the measurement station SPB-5 [m^3/min],

$q_i\,CH_4$ – methane concentration at measurement station SPB-5 [%].

By substituting the data from TABLE 5 and the determined air flow into Eq. (1), Fig. 7 we have:

$$\dot{V}_i\,CH_4 = 296.77\frac{(0.345+0.3)}{2}\,0.01 = \mathbf{0.957}\ [m^3CH_4/s] = \mathbf{57.425}\ [m^3CH_4/min]$$

3. Comparative studies

The essence of the verification study of the measurement of the volume flux of methane discharged through ventilation shaft VI was to carry out additional measurements in the four workings through which air flowed into shaft VI and then into the collecting duct of the fan station. Survey measurement stations (SPB) were located at the following locations, Fig. 8:

- SPB-1 – shaft bottom of shaft VI, level 450 m,
- SPB-2 – shaft bottom of shaft VI, level 650 m, east side,
- SPB-3 – shaft bottom of shaft VI, level 650 m, west side,
- SPB-4 – shaft bottom of shaft VI, level 850 m,
- SPB-5 – diffuser 1 of shaft VI,
- SWPPP – fan collection duct.

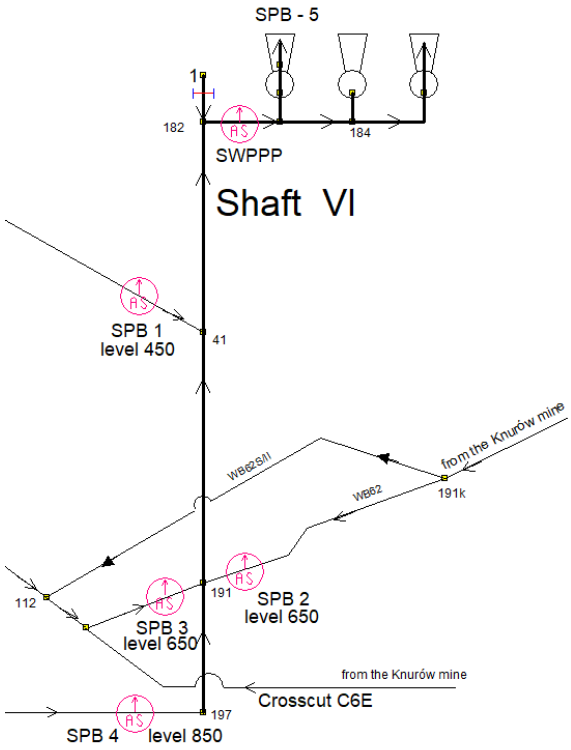

Fig. 8. Diagram of the shaft VI area, location of measurement stations at the shaft VI inlets, and in the channel and at the diffuser outlet

The location of the measurement stations was carefully chosen, with no additional obstacles causing airflow disturbances in the vicinity of the station. As a first step, the size of the cross-sectional areas at these survey measurement stations was measured using a 'laser scanner'. For this purpose, a laser rangefinder of the type Leica DISTO D810 touch [32]. The determination of the measurement stations and the measurements of the cross-sectional area of the workings at these measurement stations were carried out using the standard method and the working cross-sectional area scanning method, carried out on the same day as the measurements in the fan collection duct. To determine the size of the cross-sectional area F of each test station, standard measurements were taken:

S – width at the widest part of the working [m],
W – height in the vertical axis of the cross-section of the working W (in the support arrow) [m].

The measured values were then substituted into the formula

$$F = S \cdot W \cdot wp \tag{2}$$

where $wp = 0.8$ – a correction factor converting the area of a rectangle into an area approximating an incomplete oval [22].

Fig. 9 shows an example of the result of laser scanning measurements of the cross-sectional area of the location of station SPB-3, and TABLE 2 gives the results of the measurements and the calculated and determined magnitudes of the cross-sectional area at the other survey measurement stations obtained using the standard method and the laser scanning method.

Verification measurements to determine the amount of air and the amount of methane discharged by ventilation workings into ventilation shaft VI were carried out simultaneously with the measurements in the collecting duct. The air velocity flowing through the test stations into ventilation shaft VI was measured with µAS-4 type vane anemometers, which had valid calibration certificates from an accredited laboratory. Mean air velocity measurements using the

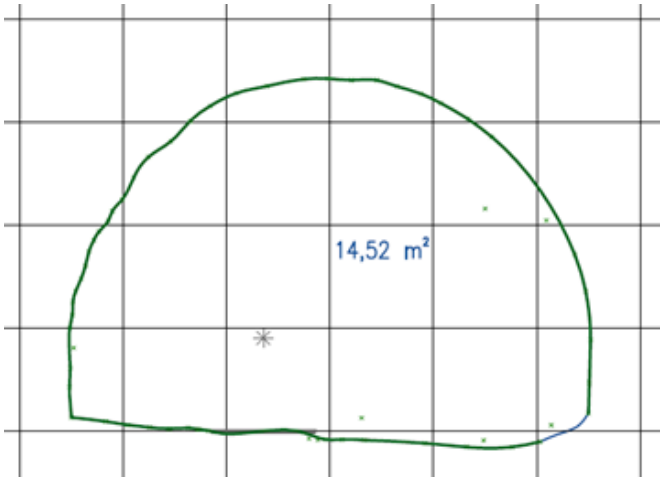

Fig. 9. Cross-sectional area at survey measurement station SPB-3 determined by laser scanning

TABLE 2

Summary of the results of cross-sectional area measurements at the survey measurement stations carried out at the four survey measurement stations

No.	Research measurement station		Size of cross-sectional area [m^2]	
	No.	Location	Standard method measurement	Measuring with a laser rangefinder, scanning
1	SPB-1	shaft bottom of shaft VI, level 450 m	13.91	13.85
2	SPB-2	shaft bottom of shaft VI, level 650 m, east side	19.58	20.73
3	SPB-3	shaft bottom of shaft VI, level 650 m, west side	14.20	14.52
4	SPB-4	shaft bottom of shaft VI, level 850 m	10.16	10.70

traverse method were taken simultaneously at each research measurement station at fixed times. Five series of measurements were taken with a time interval of 10 minutes, i.e. at 18:40, 18:50, 19:00, 19:10 and 19:20. The results of the air velocity measurements are shown in TABLE 3.

TABLE 3

Air velocity measurements at measurement stations

No.	Time	Air velocity v_i [m/s]			
		SPB-1	SPB-2	SPB-3	SPB-4
1	18:40	3.64	6.41	9.80	0.94
2	18:50	3.60	6.44	9.86	0.92
3	19:00	3.50	6.33	10.00	0.94
4	19:10	3.52	6.23	9.92	0.88
5	19:20	3.44	6.31	10.07	0.89
Average air velocity v [m/s]					
		3.54	6.34	9.93	0.91

During the measurements, the physical parameters of the flowing air were recorded at the locations of the measurement stations. The averaged results, corresponding to the same period as the volumetric flow rate measurements, are presented in TABLE 4. The determined values of the density of the flowing air will be used to calculate the volumetric flow rate converted to Nm^3. In addition, this data will allow for the determination of the mass flow rate of the flowing air, as well as the final balancing and comparison of the flow rates.

TABLE 4

Results of physical parameter measurements at the measurement station locations

Measurement station	*Ts*	*Tw*	Pressure	Air density
	[°C]	[°C]	[Pa]	[kg/m^3]
SPB-1	20.2	17.6	99869	1.178
SPB-2	24.6	22.1	102205	1.185
SPB-3	24.2	20.8	102210	1.184
SPB-4	25	21.8	104690	1.213
SPB-5	21.2	18.4	94693	1.112
Atmosphere	13.4	12.1	98052	1.186

Based on measured average air velocities v_i (TABLE 3) and the cross-sectional dimensions of the workings determined at the survey measurement stations F_i (TABLE 2), the average air flow rate Q_v flowing through these stations into ventilation shaft VI was calculated using formula (3); the results are summarised in TABLE 5.

$$Q_v = F_i \cdot v_i \cdot 60 \tag{3}$$

3.1. Comparison of flux measurements

TABLE 5 shows the results of air volumetric and mass flow rate calculations taking into account the characteristics of the anemometers, distinguishing the cross-sectional area at the test stations determined according to standard measurements of the height and width of the working (formula 2) and according to cross-sectional area measurements using laser scanning of the working. In addition, TABLE 5 summarises the results of the average value measured at the SWWPP measurement station located in the collective shaft duct, which are compared to the results of the measurements at the shaft inlets.

According to Regulation 2024/1787, the determined volumetric flow rate of the flowing air (TABLE 5) must be converted from m^3 to Nm^3 with reference to the standard conditions of temperature 273.15 K and pressure 101,325 Pa, and subsequently to mass emission, taking into account the temperature and pressure at the measurement site (TABLE 4).

The summary shows (TABLE 5) that the mass flow rate determined by the SWPPP system with SOM 2303 methane anemometers is 20.1% lower than the sum of the measured mass flow rates at the stations located at the shaft inlets.

Commenting on the result obtained, it should be noted that the measurement method using the SWPPP system takes into account the correction for velocity due to the presence of the boundary layer. The second reason for the discrepancy in the results is the influence of the contribution of

TABLE 5

Summary of the calculated volumetric and mass flow rates of the flowing air

No.	Measurement station	Average volumetric flow rate		Air density	Average volumetric flow rate normalized to standard conditions	Average mass flow
		Surface area determination method				Laser scanning method
		Standard method	Laser scanning method			
		[m^3/min]		[kg/m^3]	[Nm^3/min]	[kg/min]
—	1	2		3	4	5
1	SPB-1	2 871	2859	1.178	2624	3368
2	SPB-2	7483	7923	1.185	7333	9389
3	SPB-3	8520	8712	1.184	8075	10315
4	SPB-4	561	591	1.213	560	717
5	Total	19435	20085		18592	23789
6	Measurement in the fan collection duct [m^3/min]					
7	SPB-5 (SOM 2303)	17806	17806	1.112	15445	19800
8	Difference (5-8)	1629	2279		3146	3988
9	w %	9.1	12.8		20.4	20.1

the dynamics of the hand-held anemometer, which, when measured using the traverse method, is moved across the transverse field of the working, which can affect the measurement of the average velocity by overestimating the value of the measurement [21].

3.2. Determination of methane fluxes discharged into ventilation shaft VI

During air velocity measurements at the inlets to Shaft VI, two air samples were taken into Tedlar bags at each test measurement station, including the SPB-5 station located in the diffuser. The methane concentrations determined in the analyses are shown in TABLE 6.

TABLE 6

Summary of methane concentrations determined at test stations

No.	Research measurement station	Description of tests		CH_4 [%]	Mean concentration CH_4 [%]
		Time	Air sample bag no.		
1.	SPB-1	18:55	77	0.165	0.160
2.		19:15	78	0.155	
3.	SPB-2	18:55	83	0.255	0.2385
4.		19:15	85	0.222	
5.	SPB-3	18:55	86	0.439	0.404
6.		19:15	84	0.369	
7.	SPB-4	18:55	82	0.134	0.1285
8.		19:15	81	0.123	
9.	SPB-5	18:55	79	0.345	0.3225
10.		19:15	80	0.300	

According to the regulations in force, the amount of methane in mine air $\dot{V}_i$ CH_4 is calculated according to formula (1). TABLE 7 provides a summary of the amount of methane at the test stations for the specified average air flow rate values (TABLE 5).

TABLE 7

Summary of methane quantities at test stations depending on how the cross-sectional area is measured

No.	Measurement station	Average CH_4 concentration [%]	Average amount of methane [m^3CH_4/min], by method speed measurements by anemometer	
			Cross-sectional area standard method	Cross-sectional area by laser scanning
1	SPB-1	0.1600	4.5936	4.5744
2	SPB-2	0.2385	17.8469	18.8963
3	SPB-3	0.4040	34.4208	35.1964
4	SPB-4	0.1285	0.7208	0.7594
5		Total	57.5821	59.3265

The table above (TABLE 7) shows that the total measured volume of methane flowing into ventilation shaft VI of the mine also depends on the method adopted for measuring the cross-sectional area.

It is interesting to compare the methane flux values determined using the SWPPP measurement system:

$$\dot{V}_i\,CH_4 = \mathbf{0{,}957}\ [m^3CH_4/s]$$

in relation to the values determined by measuring at the inlets to shaft VI by the most accurate method of measuring the cross-section, which is:

$$\dot{V}_i\,CH_4 = \mathbf{0{,}98877}\ [m^3CH_4/s]$$

The methane flux determined using the SWPPP air volume measurement system (reference measurement) and the methane value measured at station SPB-5 is lower by 0.03169 m^3CH_4/s, 0.03524 $kgCH_4/s$] than the total flux determined at the shaft inlets.

A numerical example illustrating the effects of such a difference is as follows:

- For the volumetric flow rate: 114.1 m^3CH_4/hour, 2,738.2 m^3CH_4/day, and 999,376 m^3CH_4/year,
- For the mass flow rate: 126.9 $kgCH_4$/hour, 3,044.7 $kgCH_4$/day, and 1,111.3 tons CH_4/year.

3.3. Analysis of measurement uncertainty

An important issue in ventilation metrology is the determination of measurement uncertainty, which should be an integral part of every measurement session. Measurement uncertainty is a parameter associated with the measurement result, characterising the spread of values and informing us about the errors involved in conducting the measurements. This leads to a better understanding of the level of hazards, such as methane or temperature-related risks, associated with the measured ventilation parameter.

3.3.1. Methods for measuring methane flow rate

The presented methods for measuring the methane flow rate belong to the group of composite measurements, whose results depend on the measurement of geometric dimensions, average flow velocity, and average methane concentration across the cross-section of the gallery. Each of these measurements constitutes a separate metrological issue and should be considered according to the applied method.

3.3.2. Volumetric flow rate measurement using the reference method with SWPPP

The reference method adopted in this article for determining the volumetric flow rate is based on measuring instantaneous flow velocities at a finite number of points within a plane corresponding to the cross-section of the gallery. Using a gridding method, a dense mesh of values is obtained based on linear triangulation. This leads to dividing the gallery cross-section into triangles with known areas, within which partial volumetric flow rates are calculated. Velocity values at boundary points are determined based on prior analyses of velocity profile distributions near the roof and floor. Applying this method requires specifying the position of anemometers in a cartesian coordinate system related to the measurement cross-section. This method, along

with its uncertainty estimation, is described in detail in [14]. In the analysed measurement case, the obtained relative expanded uncertainty at a 95% confidence level ($k = 2$) for determining the volumetric flow rate of the air-methane mixture was 5.2%.

3.3.3. Measurement of gallery cross-sectional area – standard method (tape measure)

The commonly accepted method for measuring the cross-sectional area of mining galleries, used by underground ventilation services, is the tape method. This method is primarily used for galleries supported with arched supports of the ŁP type. It involves measuring the width of the gallery at a height of 30 to 50 cm above the floor and the height of the mining support. The cross-sectional area is calculated as the product of width, height, and a coefficient related to the shape of the support. For arched supports, the coefficient is assumed to be 0.8. The relative expanded uncertainty ($k = 2$) of such a measurement does not exceed 3% of the measured value, provided that the cross-section of the support is undeformed and there is no floor heaving [9].

3.3.4. Measurement of gallery cross-sectional area using 3D scanners

3D scanners based on LiDAR technology are gaining increasing significance in mining surveying – especially in underground mines. One of their applications is measuring gallery cross-sections to create precise models of cross-sectional and longitudinal profiles, compare actual conditions with designs, and monitor rock deformations and displacements [24]. Examples include the measurements presented in [11], where the authors focus on using 3D scanning as a reference method for determining the cross-sectional area of mining galleries. The accuracy of measurements using this technology in field conditions has been studied extensively, e.g., in [12], which confirmed the metrological parameters declared by scanner manufacturers under industrial conditions, and [28], which describes sources of errors in the context of industrial measurements. However, the authors of this article did not find publications describing uncertainty estimation methods applicable to measuring the cross-sectional area of ventilation ducts, including mining galleries.

3.3.5. Measurement of average flow velocity – continuous traverse method

Mining ventilation practice assumes measuring the average flow velocity using the continuous traverse method. This method involves slowly moving an anemometer at a constant speed along a selected trajectory within the cross-section of the mining gallery while simultaneously recording local velocity values at a chosen frequency. The average flow velocity is calculated based on the collected data. The measurement result is subject to uncertainty influenced by factors such as the anemometer's metrological properties (instrument accuracy), air fluctuations, shape of the traverse path, anemometer movement speed, velocity profile, and the presence of the person performing the measurement near the gallery cross-section. The influence of these parameters on the average flow velocity measurement results and the principles of creating an uncertainty budget for this type of measurement are detailed in [7]. Based on this, the estimated relative expanded uncertainty ($k = 2$) in the analysed case did not exceed 5%.

3.3.6. Measurement of average methane concentration

In the presented experimental measurement, methane concentration was determined using chromatographic analysis. Gas samples were collected over a specified time at measurement cross-sections and subsequently sent to a laboratory for analysis. Estimating uncertainty for this type of analysis involves identifying uncertainty sources. According to [2], the most significant factors affecting chromatographic analysis results include operating conditions (operators, environmental conditions, etc.), detector properties (drift, signal noise, etc.), calibration, preparation of standards and samples, analyte stability, measurement repeatability, and sample preparation. Taking all these factors into account, the relative expanded uncertainty at a 95% confidence level ($k = 2$) for methane concentration determination in air-methane mixtures, achieved by leading laboratories, is approximately 0.1%. This applies to methods for certifying standard gas mixtures. For standard procedures used in routine analyses, the uncertainty level reaches several percent to over ten percent.

3.3.7. Measurement of methane volumetric flow rate

A comprehensive study on methane volumetric flow rate measurement using basic methods routinely applied in mining is presented in [7]. The authors demonstrate a high variability in the relative uncertainty of this type of measurement, depending on air flow velocity and average methane concentration – reaching up to 160% for the lowest velocities and concentrations (0.5 m/s and 0.1% CH_4). As velocity and concentration increase, the relative uncertainty decreases to about 15% (5 m/s, 20% CH_4). These results highlight the challenges of performing such measurements, especially when approaching the lower detection limits of the instruments and methods used.

4. Summary

Measurement of the average air velocity in the working fan section in mining practice is most often carried out with a vane anemometer using the continuous traverse method. The advent of new measurement systems brings new opportunities in ventilation measurement. As analysis of the literature shows, the pulsation of air velocity has the greatest influence on the measurement result. This is also confirmed by the results of research conducted by [7,16,21]. The presence of an observer in the working environment also has a significant impact on the measurement. There is less impact of traverse speed, and when using anemometers with any averaging time that allows traversing at low speed, the impact of this speed on the measurement result can be negligibly small compared to the impact of the other factors.

When analysing the collected test results for the determination of the flux, it should be emphasised that performing a correct measurement of the velocity and measuring the cross-sectional area requires the operator to be diligent and patient in following the rules of the measurement procedures.

As part of the measurement experiments, control measurements of air velocity and methane concentration were made with the SWPPP multipoint system in the ventilation duct of shaft VI, together with air and methane sampling from the fan diffuser. The determined average flow rate for the period 18:40:02 to 19:20:12 was $Q_v = 296.77$ m^3/s (17806 m^3/min).

Based on the determined volume flow rate of the flowing air Q_v (Fig. 7) and the methane concentration measured at measurement station SPB-5, the volume flux of $V_i\,CH_4$ flowing out through shaft VI was calculated, which was **57.425** [m^3CH_4/min] and which is 3.3% lower than the value determined at the shaft inlets.

Calculations performed of methane flow rates at the test stations for the specified average air flow rate values (TABLE 5), indicate that the measured total amount of methane flowing into ventilation shaft VI depends on the method adopted for measuring the cross-sectional area and for the traverse method (TABLE 7).

TABLE 5 summarises the results of the flow rate measurements at the measurement stations at the inlets to shaft VI, which are compared to the average value measured at the measurement station located in the collective shaft duct.

These values were converted to Nm^3 as well as to the mass flow rate of the flowing air-methane mixture (TABLE 5). A comparison of the flow rates determined by the SWPPP system with the sum of values measured at stations located at the air inlets to the shaft shows that:

- the volumetric flow rate is lower by 12.8%,
- the volumetric flow rate converted to Nm^3 is lower by 20.4%,
- the mass flow rate is lower by 20.1%.

The discrepancies in the results are due to the influence of airflow velocity pulsations and the dynamics of the anemometer, which tends to overestimate the average velocity when using the traverse method [21, 23].

Taking into account the available methods and measuring instruments useful for the determination of the volume flux of flowing air in the mine workings [9,14,23], it is recommended to use a multipoint system for the measurement of velocity and methane concentration together with SOM 2303-type methanoanemometers. Enhancing the SWPPP system with multipoint synchronous methane concentration measurement creates a metrological system that enables the study of methane concentration distributions at the measurement site and the observation of methane concentration transients at region outlets or in the fan duct.

Based on the measurements of air and methane fluxes in the collective duct of the fan station on shaft VI, a measurement uncertainty budget will be developed, and the results will be presented in a separate publication. It is expected that due to the layout of 16 identical measuring instruments, evenly distributed (Photo 1.) in the measuring section, measuring the air flow rate at the same time, the determined uncertainty of the air flow rate measurement will be within 5%. Due to the humidity of the flowing air and the continuous measurement, especially of the methane concentration, with an instrument of the SOM 2303 type (pellistor methane sensor), measurement in a duct or on a diffuser will not always meet the requirements, due to the measuring range of the methane sensor and the possibility of periodic condensation of the water vapor contained in the flowing air from the mine.

References

[1] T. Andersen, Z. Zhao, M. Vries, J. Neck, J. Swolkien, M. Menoud, T. Röckmann, A. Roiger, A. Fix, W. Peters, H. Chen, Local-to-regional methane emissions from the Upper Silesian Coal Basin (USCB) quantified using UAV-based atmospheric measurements. Atmos. Chem. Phys. **23**, 5191-5216 (2023). DOI: https://doi.org/10.5194/acp-23-5191-2023

[2] Alicia Maroto, Ricard Boqué, Yvan Vander Heyden Estimating Uncertainty LCGC Europe **21** (12), 628 (2008).

[3] B. Belle, Real-time air velocity monitoring in mines – A quintessential design parameter for managing major mine health and safety hazards. In 13th Coal Operators' Conference; Aziz, N., Ed.; University of Wollongong: Wollongong, Australia, 2013; pp. 184-198.

[4] I. Care, F. Bonthous, J.R. Fontaine, Measurement of air flow in duct by velocity measurements. In: 16th international congress of metrology, October 7-10 2013, Paris, France.

[5] E. Chiuzan, G.A. Găman, D. Cioclea, C. Tomescu, I. Gherghe, Continuous invasive monitoring technology for determination of air velocity at the level of main ventilation station. Environmental Engineering and Management Journal **18**, 4, 789-795 (2019). DOI: https://doi.org/10.30638/eemj.2019.073

[6] W. Dziurzyński, A. Krach, Pole prędkości przepływu powietrza w kanale kopalnianej stacji wentylatorowej. Archiwum Górnictwa **46**, 3 (2002).

[7] W. Dziurzyński, A. Krach, S. Wasilewski, Wyznaczanie niepewności pomiaru parametrów fizyko-chemicznych powietrza w kopalniach głębinowych. Monografia 2013 rok. Instytut Mechaniki Górotworu Polskiej Akademii Nauk s. 91 (2013).

[8] W. Dziurzyński, M. Gawor, T. Pałka, Wyznaczanie profilu prędkości przepływu powietrza w wyrobisku górniczym – narzędzia informatyczne. Wydawnictwo Instytut Mechaniki Górotworu PAN, 2016, Monografia, ISBN 978-83-946392-2-8.

[9] W. Dziurzyński i in., Zasady pomiarów przepływu powietrza w wyrobiskach kopalnianych. Wybrane sposoby kontroli i kalibracji przyrządów pomiarowych. Rozprawy, Monografie, Wydawnictwo IMG PAN, 2017 nr 10, ISBN 978-83-929976-6-5.

[10] J. Janus, J. Krawczyk, J. Kruczkowski, P. Ostrogórski, Nowe rozwiązania urządzeń do pomiaru pól prędkości i rozkładów stężenia metanu oraz wyniki badań porównawczych. Prace Instytutu Mechaniki Górotworu PAN **14**, 1-4, 149-163 (2012).

[11] J. Janus, P. Ostrogórski, Underground Mine Tunnel Modelling Using Laser Scan Data in Relation to Manual Geometry Measurements. Energies **15**, 2537 (2022). DOI: https://doi.org/10.3390/en15072537

[12] T.P. Kersten, M. Lindstaedt, Geometric accuracy investigations of terrestrial laser scanner systems in the laboratory and in the field. Appl. Geomat. **14**, 421-434 (2022). DOI: https://doi.org/10.1007/s12518-022-00442-2

[13] A. Krach, J. Krawczyk J. Kruczkowski, T. Pałka, Zmienność pola prędkości i strumienia objętości powietrza w wyrobiskach kopalń głębinowych. Arch. Min. Sci., Monograph 1, Kraków 2006.

[14] A. Krach, Uncertainty of measurement of selected mine ventilation parameters. (Niepewność pomiaru wybranych wielkości w kopalnianych pomiarach wentylacyjnych). Archives of Mining Sciences, Monograph No 8, (2009), ISSN 0860-7001, s. 147.

[15] J. Krawczyk, P. Ligęza, E. Poleszczyk, P. Skotniczny, Advanced hot-wire anemometric measurment systems in investigations of the air flow velocity fields in mine headings. Arch. Min. Sci. **56**, 4, 683-700 (2011).

[16] J. Kruczkowski, Wpływ własności dynamicznych czujnika anemometru skrzydełkowego na dokładność pomiaru prędkości przepływu powietrza. Praca doktorska, IMG PAN, Kraków 1999.

[17] J. Kruczkowski, Wyznaczanie metanowości wentylacyjnej przy wykorzystaniu nowej techniki pomiarowej. Materiały 7 Szkoły Aerologii Górniczej, Krynica-Zdrój, 9-11 październik 2013, s. 71-82.

[18] J. Kruczkowski, P. Ostrogórski, Metanoanemometr SOM 2303. Materiały 8 Szkoły Aerologii Górniczej w Jaworze 13÷16 października 2015.

[19] J. Kruczkowski, P. Ostrogórski, New Method for Ventilation Methane Content Monitoring. Proceedings of the 11th International Mine Ventilation Congress (2018). DOI: https://doi.org/10.1007/978-981-13-1420-9_23

[20] A.L. Martikainen, H.N. Dougherty, C.D. Taylor, A.L. Mazzella, Sonic anemometer airflow monitoring technique for use in underground mines. In: Proceedings of the 13th U.S./North American mine ventilation symposium, Sudbury, Ontario, Canada, June 13-17 McPherson MJ (2009).

[21] P. Ostrogórski, Właściwości dynamiczne cyfrowego anemometru skrzydełkowego. Przegląd Górniczy **71**, 4 (2015).

[22] P. Ostrogórski, Consideration of the shape and height of the floor in result of measuringthe cross-sectional area for rings type ŁP (Uwzględnienie kształtu i wysokości spągu w wyniku pomiaru pola przekroju dla obudowy typu ŁP). Prace Instytutu Mechaniki Górotworu PAN **17**, nr 1-2, 27-30 (2015).

[23] P. Ostrogórski, Metoda trawersu ciągłego w pomiarze prędkości średniej powietrza anemometrem skrzydełkowym. Materiały 9 Szkoły Aerologii Górniczej (2017).

[24] G.C. Rhoderick, Analysis of natural gas: the necessity of multiple standards for calibration. J. Chromatogr. A. **31**, 1017 (1-2) 131-9 (2003). DOI: https://doi.org/10.1016/j.chroma.2003.08.002. PMID: 14584698

[25] Rozporządzenie Parlamentu Europejskiego i Rady (UE) 2024/1787 z dnia 13 czerwca 2024 roku w sprawie redukcji emisji metanu w sektorze energetycznym. http://data.europa.eu/eli/reg/2024/1787/oj

[26] S. Kumar Singh, B. Pratap Banerjee, S. Raval, A review of laser scanning for geological and geotechnical applications in underground mining. International Journal of Mining Science and Technology **33**, 2, 133-154 (2023). DOI: https://doi.org/10.1016/j.ijmst.2022.09.022

[27] P Skotniczny, P. Ostrogórski, Three-dimensional air velocity distributions in the vicinity of a mine heading's sidewall. Arch. Min. Sci. **63**, 2, 335-352 (2018). DOI: https://doi.org/10.24425/122451

[28] A. Suresh, A. Mathew, P.B. Dhanish, Factors influencing the measurement using 3D laser scanner: A designed experimental study. J. Mech. Sci. Technol. **38**, 5605-5615 (2024).
DOI: https://doi.org/10.1007/s12206-024-0931-1

[29] J. Swolkień, Polish underground coal mines as point sources of methane emission to the atmosphere. International Journal of Greenhouse Gas Control **94**, 102921 (2020). DOI: https://doi.org/10.1016/j.ijggc.2019.102921

[30] J. Swolkień, A. Fix, M. Gałkowski, Factors influencing the temporal variability of atmospheric methane emissions from Upper Silesia coal mines: a case study from the CoMet mission. Atmos. Chem. Phys. **22**, 16031-16052 (2022). DOI: https://doi.org/10.5194/acp-22-16031-2022

[31] S. Trenczek, P. Wojtas, Rozwój monitorowania zagrożeń naturalnych w okresie ostatniego 20-lecia (Development of natural hazard monitoring over the last 20 years). Bezpieczeństwo Pracy I Ochrona środowiska w Górnictwie **9**, 3-10 (2014).

[32] User manual Leica Disto D810 touch, User manual Leica Disto D810 touch (English, 44 pages).

[33] L. Zhou, R.A. Thomas, L. Yuan, D. Bahrami, Experimental Study of Improving a Mine Ventilation Network Model Using Continuously Monitored Airflow. Mining, Metallurgy & Exploration **39**, 887-895 (2022).
DOI: https://doi.org/10.1007/s42461-022-00574-4

[34] L. Zhou, L. Yuan, R.A. Thomas, Iannacchione, Determination of velocity correction factors for real-time air velocity monitoring in underground mines. International Journal of Coal Science and Technology **4**, 322-332 (2017).
DOI: https://doi.org/10.1007/s40789-017-0184-z